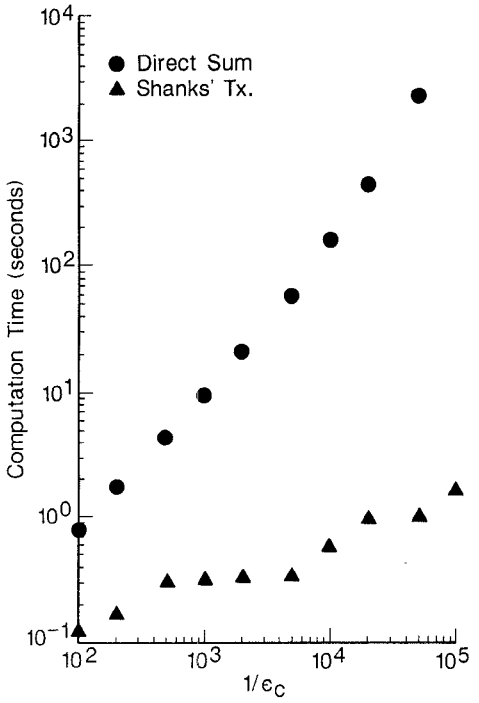

Fig. 8. Computation time in seconds versus $1/\epsilon_c$ for the case in Fig. 7.

terms and takes 2400 s to compute. The saving factor for this case is 2667.

IV. Conclusion

The series representing the free-space periodic Green's function has been accelerated by a simple application of Shanks's transform. Higher order transforms are easily computed via Wynn's ϵ algorithm. It has been shown that the computation time can be reduced by a factor of a few hundreds and, in some instances, a few thousands. This is a significant reduction in computation time as the Green's function is evaluated repeatedly in a moment method solution. The transform is very simple to implement and is extremely efficient, as shown by the numerical results.

References

[1] S. Singh, W. F. Richards, J. R. Zinecker, and D. R. Wilton, "Accelerating the convergence of series representing the free space periodic Green's function," *IEEE Trans. Antennas Propagat.*, vol. 38, pp. 1958–1962, Dec. 1990.

[2] S. Singh and R. Singh, "Application of transforms to accelerate the summation of periodic free- space Green's functions," *IEEE Trans. Microwave Theory Tech.*, vol. 38, pp. 1746–1748, Nov. 1990.

[3] R. Lampe, P. Klock, and P. Mayes, "Integral transforms useful for the accelerated summation of periodic, free-space Green's functions," *IEEE Trans. Microwave Theory Tech.*, vol. MTT-33, pp. 734–736, Aug. 1985.

[4] R. E. Jorgenson and R. Mittra, "Efficient calculation of the free-space periodic Green's function," *IEEE Trans. Antennas Propagat.*, vol. 38, pp. 633–642, May 1990.

[5] R. E. Jorgenson and R. Mittra, "Oblique scattering from lossy strip structures with one- dimensional periodicity," *IEEE Trans. Antennas Propagat.*, vol. 38, pp. 212–219, Feb. 1990.

[6] W. F. Richards, K. McInturff, and P. S. Simon, "An efficient technique for computing the potential Green's function for a thin, periodically excited parallel plate waveguide bounded by electric and magnetic walls," *IEEE Trans. Microwave Theory Tech.*, vol. MTT-35, pp. 276–281, Mar. 1987.

[7] S. Singh and R. Singh, "On the use of Shanks's transform to accelerate the summation of slowly converging series," *IEEE Trans. Microwave Theory Tech.*, vol. 39, pp. 608–610, Mar. 1990.

[8] D. Shanks, "Non-linear transformations of divergent and slowly convergent sequences," *J. Math. Phys.*, vol. 34, pp. 1–42, 1955.

[9] P. Wynn, "On a device for computing the $e_m(S_n)$ transformation," *Math. Tables Other Aids Comput.*, vol. 10, pp. 91–96, 1956.

[10] B. A. Munk and G. A. Burrell, "Plane-wave expansion of arrays of arbitrarily oriented piecewise linear elements and its application to determining the impedance of a single linear antenna in a lossy half-space," *IEEE Trans. Antennas Propagat.*, vol. AP-27, pp. 331–343, May 1979.

Capacitance of a Circular Symmetric Model of a Via Hole Including Finite Ground Plane Thickness

Peter Kok and Daniël De Zutter

Abstract—**The capacitance of a simplified model of a via hole is calculated based on an integral equation approach for the surface charge density. The finite ground plane thickness is explicitly taken into account. Numerical data are obtained for a large range of realistic geometrical data. The relative importance of the contribution to the total capacitance coming from the ground plane opening is explicitly evaluated. It is found that the via capacitance is proportional to the square root of its height, at least for the range of geometrical data considered in this paper.**

I. Introduction

Microstrips and striplines in printed circuit board (PCB) technology for high-frequency/high-speed controlled impedance transport of signals have been extensively studied and modeled [1]. This is much less the case for printed wire technology such as Multiwire® or Microwire® [2], [3]. The parasitic effects caused by discontinuities present in both technologies, such as line crossings, pads, lands, and via holes, form a quite important and still relatively new research topic [4], [5].

In this paper attention is focused on the capacitance of via holes. Via holes provide the connection between lines located in different layers of a multilayered board and therefore have to cross at least one ground plane. Measurements clearly indicate that the effect of realistic via holes is mainly capacitive.

Earlier publications [6], [7] calculate the capacitance and inductance of vias between two different lines above the same ground plane. In [8], capacitance and inductance are calculated for a via hole crossing an infinitely thin ground plane. In this paper, the capacitance of a via hole crossing a ground plane with finite thickness is calculated. To simplify the analysis we have neglected the lines connected by the via.

The formulation of the problem is based on an integral equation for the surface charges combined with an analytical solution at the ground plane opening. The behavior of the via hole capacitance is explicitly studied in terms of the geometrical

Manuscript received July 16, 1990; revised February 11, 1991.

The authors are with the Laboratory for Electromagnetism and Acoustics, University of Ghent, Sint Pietersnieuwstraat 41, 9000 Ghent, Belgium.

IEEE Log Number 9100142.

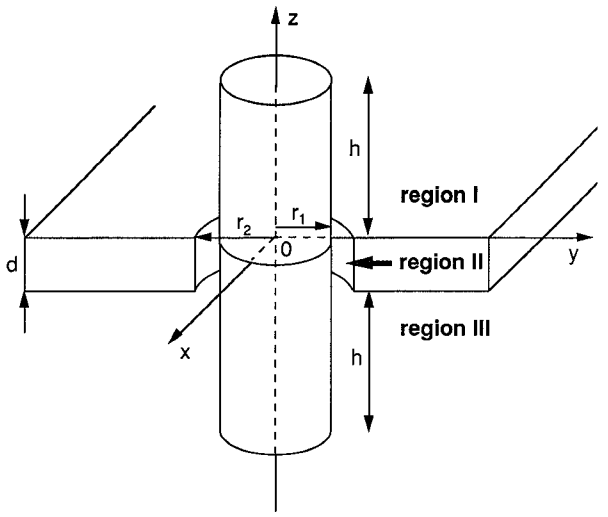

Fig. 1. Geometry of the problem.

parameters which govern the problem, and the contribution coming from the finite ground plane thickness is clearly identified.

II. Formulation of the Problem

The geometry of the problem is shown in Fig. 1. As emphasized in the Introduction, we use a simplified model of a via hole consisting of a perfectly conducting cylinder of finite height $2h + d$. The cylinder passes through a ground plane with finite thickness d, pointing out of the plane at both sides over a distance h. Its radius is r_1; the radius of the ground plane opening is r_2. No wires or microstrips are attached to preserve the circular symmetry of the problem. The entire structure is symmetric with respect to the plane $z = -d/2$. It is embedded in a homogeneous dielectric with dielectric constant ϵ.

It is our purpose to calculate the capacitance of this via hole model and, in particular, to determine the influence of its radius r_1, its height h, and the radius r_2 of the ground plane opening. To this end, the potential at the cylinder is chosen to be V; the potential at the ground plane is zero. The capacitance of the cylinder is then calculated as the total surface charge density on the cylinder divided by V. The proposed solution of the capacitance problem is analytical at the passage through the ground plane (region II) and numerical above (region I) and under the ground plane (region III), where an integral equation is solved. The different regions are connected through appropriate boundary conditions.

We now present some details of the solution in each region.

III. Analytical Solution at the Passage Through the Ground Plane

In region II (see Fig. 2), which is the region enclosed by the cylindrical surface of the inner conductor ($r = r_1$), the opening in the ground plane ($r = r_2$), and the planes $z = 0$ and $z = d$, the potential ϕ satisfies Poisson's equation subject to the following boundary conditions:

$$\phi = 0 \qquad \text{at } r = r_2$$

$$\phi = V \qquad \text{at } r = r_1. \tag{1}$$

At the symmetry plane $z = -d/2$, the electric field has only a radial component. This is expressed by an additional condition on ϕ:

$$\frac{\partial \phi}{\partial z} = 0 \qquad \text{at } z = -\frac{d}{2}. \tag{2}$$

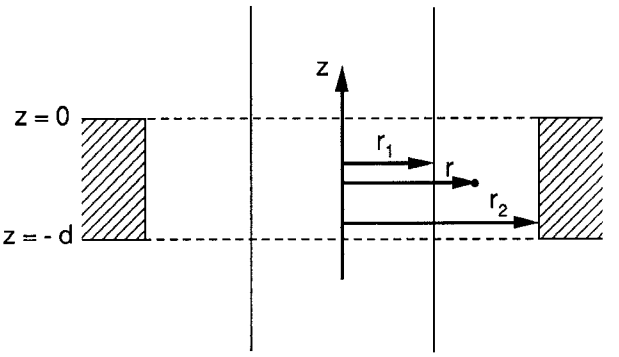

Fig. 2. Detail of the ground plane opening.

Owing to the circular symmetry around the z axis, the solution of Poisson's equation is only r- and z-dependent. Separation of variables [9] and conditions (1) and (2) lead to

$$\frac{\phi}{V} = \frac{\ln \dfrac{r}{r_2}}{\ln \dfrac{r_1}{r_2}} + \sum_{n=1}^{\infty} A_n \cosh\left[\alpha_n\left(z + \frac{d}{2}\right)\right] F_{0n}(r, r_1) \tag{3}$$

where

$$F_{0n}(v, w) = J_0(\alpha_n v) Y_0(\alpha_n w) - Y_0(\alpha_n v) J_0(\alpha_n w). \tag{4}$$

The constants A_n will be determined below. They express the influence of regions I and III on the solution for region II. J_0 and Y_0 are the zeroth-order Bessel functions of the first and second kinds. α_n are the eigenvalues of the problem and can be found as solutions of

$$F_{0n}(r_1, r_2) = 0. \tag{5}$$

IV. Integral Equation Solution in the Upper and Lower Half Space

In regions I and III, the potential ϕ will be found as the solution of an integral equation. Since the solutions in regions I and III are symmetric with respect to the plane $z = -d/2$, we need only to find the solution in region I.

In order to take advantage of the circular symmetry around the z axis, the appropriate integral equation will be based on a Green's function, G, that exhibits the same circular symmetry. To determine this Green's function, we start from the static Green's function, G_0, for the homogeneous half-space bounded by a perfectly conducting plane at $z = 0$:

$$G_0(\vec{r}, \vec{a}) = -\frac{1}{4\pi\epsilon}\left(\frac{1}{|\vec{r} - \vec{a}|} - \frac{1}{|\vec{r} - \vec{a}'|}\right). \tag{6}$$

Here, $\vec{r}$ represents the position vector of the observation point. It can be written in Cartesian coordinates (x, y, z) or cylindrical coordinates (r, θ, z). $\vec{a}$ represents the position vector of the source point. Its Cartesian coordinates will be called (a, b, c), its cylindrical coordinates (r_a, θ_a, c). $\vec{a}'$ is the image of $\vec{a}$ with respect to the plane $z = 0$; hence its coordinates are given by $(a, b, -c)$ or $(r_a, \theta_a, -c)$.

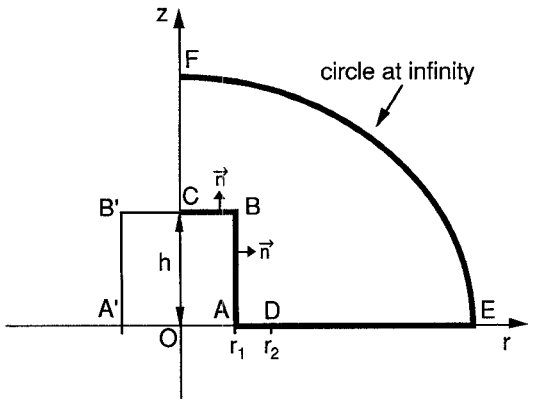

Fig. 3. Relevant to the integral equation above the ground plane.

The Green's function, G, is determined as

$$G(\vec{r}, r_a, c) = \int_0^{2\pi} G_0(\vec{r}, \vec{a})\, d\theta_a = -\frac{1}{\pi\epsilon}\frac{K(k_1)}{R_1} + \frac{1}{\pi\epsilon}\frac{K(k_2)}{R_2} \tag{7}$$

with $K(k)$ the complete elliptic integral of the first kind [10] and

$$R_1 = \sqrt{(z-c)^2 + (r+r_a)^2}$$

$$R_2 = \sqrt{(z+c)^2 + (r+r_a)^2}$$

$$k_1 = \frac{2\sqrt{rr_a}}{R_1}$$

$$k_2 = \frac{2\sqrt{rr_a}}{R_2}. \tag{8}$$

In the upper half-space, i.e., $z \geq 0$ and $c \geq 0$, G and ϕ satisfy the following equations:

$$\nabla^2 G = \frac{1}{r_a \epsilon}\delta(r - r_a)\delta(z - c) \tag{9}$$

$$\nabla^2 \phi = 0 \tag{10}$$

with

$$\nabla^2 = \frac{1}{r_a}\frac{\partial}{\partial r_a}\left(r_a \frac{\partial}{\partial r_a}\right) + \frac{\partial^2}{\partial c^2}. \tag{11}$$

After multiplying (9) by ϕ and (10) by G and subtracting the results, we apply Green's theorem to the upper half-space, $z > 0$. Because of the circular symmetry, surface integrations are reduced to line integrations along the bold line of Fig. 3. Taking into account that G vanishes along OE, we obtain the following integral equation:

$$\phi(\vec{r}) = -V\epsilon \int_{OA} r_a \frac{\partial G}{\partial c}(c=0)\, dr_a - \epsilon \int_{AD} r_a \phi(r_a, c=0)\frac{\partial G}{\partial c}(c=0)\, dr_a - \int_{ABC} \sigma r_a G\, dl_a. \tag{12}$$

The last term expresses the contribution of the surface charge densities, with $dl_a = dc$ along AB and $dl_a = dr_a$ along BC. The presence of σ in this term originates from the equivalence $\partial\phi/\partial n = -\sigma/\epsilon$ on a perfect conductor. The first term of (12) vanishes only when the total conductor surface, $ABB'A'$, would be closed, which is not the case in this problem (the integrating surface stops at the hole in the ground plane). The second term of (12) expresses the presence of the hole in the ground plane. The derivative $\partial/\partial c$ is the derivative with respect to the z coordinate of the source point (r_a, θ_a, c).

A second equation is needed to express the continuity of the dielectric displacement at the transition between the upper half-space (I) and the hole (II). As the dielectric constant remains the same, this amounts to

$$\frac{\partial \phi_{\mathrm{I}}}{\partial z}(z = 0+) = \frac{\partial \phi_{\mathrm{II}}}{\partial z}(z = 0-). \tag{13}$$

The left-hand side of (13) is found by deriving (12) with respect to z. The right-hand side is the first-order z derivative of (3). This leads to

$$-V\sum_{n=1}^{\infty} A_n \alpha_n \sinh\left(\alpha_n \frac{d}{2}\right) F_{0n}(r, r_1) = V\epsilon \int_{OA} r_a \frac{\partial^2 G}{\partial z \partial c}(c=0)\, dr_a + \epsilon \int_{AD} r_a \phi(r_a, c=0)\frac{\partial^2 G}{\partial z \partial c}(c=0)\, dr_a + \int_{ABC} r_a \frac{\partial G}{\partial z}\sigma\, dl_a. \tag{14}$$

Equations (12) and (14) are the coupled integral equations that have to be solved. The unknowns are the constants A_n and the surface charge distribution, σ. The attention of the reader is drawn to the presence of the double derivatives in (14). The difficult self-patch calculation caused by this presence will be discussed in Section V.

V. Numerical Implementation of the Solution

To solve (12) and (14) we use the method of moments in conjunction with point matching. To this end, AB and CB are divided into, respectively, M and N equal-length intervals and σ is taken to be constant in each interval. We impose (12) at the center of these intervals.

The number of unknown coefficients A_n in (3) is restricted to L. We impose (14) in at least L points equally spaced between A and D. Numerical experiments show that it is better to impose (14) in a number of points exceeding L.

The above approach leads to a discretized set of equations, which is then solved in a least-squares sense. The discretized version of (12) is

$$\sum_{i=0}^{N-1} \tau_i T_i(r, z) + r_1 \sum_{j=0}^{M-1} \sigma_j S_j(r, z) + \epsilon V \sum_{n=1}^{L} A_n X_n(r, z) = VB(r, z) \tag{15}$$

with

$$T_i(r,z)=\int_{r_i}^{r_{i+1}} r_a G(c=h)\,dr_a \tag{16}$$

$$S_j(r,z)=\int_{z_j}^{z_{j+1}} G(r_a=r_1)\,dc \tag{17}$$

$$X_n(r,z)=\int_{r_1}^{r_2} r_a \frac{\partial G}{\partial c}(c=0)\cosh\left(\alpha_n\frac{d}{2}\right)F_{0n}(r_a,r_1)\,dr_a \tag{18}$$

$$B(r,z)=-\epsilon\int_0^{r_1} r_a\frac{\partial G}{\partial c}(c=0)\,dr_a - \epsilon\int_{r_1}^{r_2} r_a\frac{\partial G}{\partial c}(c=0)\frac{\ln\dfrac{r}{r_2}}{\ln\dfrac{r_1}{r_2}}\,dr_a-1. \tag{19}$$

On the right-hand side of (12), we have replaced $\phi(r_a,c=0)$ with its value given in (3). On the left-hand side, $\phi(\vec{r})$ was replaced with its imposed value, V. An elementary interval along CB is defined by $[r_i,r_{i+1}]=[i(r_1/N),(i+1)(r_1/N)]$, with $c=h$ and $i=1,2,\cdots,N$. The constant surface charge density in one such interval is denoted by τ_i. Line AB is divided in M intervals $[z_j,z_{j+1}]=[j(h/M),(j+1)(h/M)]$, with $r_a=r_1$ and $j=1,2,\cdots,M$. The constant surface charge density in one such interval is denoted by σ_j. We impose (15) in the midpoints of CB, i.e., $r_{im}=(r_i+r_{i+1})/2$ and $z=h$, and in the midpoints of AB, i.e., $z_{jm}=(z_j+z_{j+1})/2$ and $r=r_1$. The discretized version of (14) becomes

$$\sum_{i=0}^{N-1}\tau_i P_i(r)+r_1\sum_{j=0}^{M-1}\sigma_j Q_j(r)+V\epsilon\sum_{n=1}^{L}A_n W_n(r)=V\epsilon D(r) \tag{20}$$

with

$$P_i(r)=\epsilon^2\int_{r_i}^{r_{i+1}} r_a\frac{\partial G}{\partial z}(c=h,\ z=0)\,dr_a \tag{21}$$

$$Q_j(r)=\epsilon^2\int_{z_j}^{z_{j+1}}\frac{\partial G}{\partial z}(r_a=r_1,\ z=0)\,dc \tag{22}$$

$$W_n(r)=\epsilon\alpha_n\sinh\left(\alpha_n\frac{d}{2}\right)F_{0n}(r,r_1) + \epsilon^2\int_{r_1}^{r_2} r_a\frac{\partial^2 G}{\partial z\partial c}(c=0,\ z=0)\cdot\cosh\left(\alpha_n\frac{d}{2}\right)F_{0n}(r_a,r_1)\,dr_a \tag{23}$$

$$D(r)=-\epsilon^2\left(\int_0^{r_1} r_a\frac{\partial^2 G}{\partial z\partial c}(c=0,\ z=0)\,dr_a + \int_{r_1}^{r_2} r_a\frac{\ln\dfrac{r_a}{r_2}}{\ln\dfrac{r_1}{r_2}}\frac{\partial^2 G}{\partial z\partial c}(c=0,\ z=0)\,dr_a\right). \tag{24}$$

We impose (20) in L' equally spaced points along AD, i.e., $r=r_1+(p+1/2)(r_2-r_1)/L'$, with $p=0,1,\cdots,L'-1$. L' must be larger than or equal to L.

As long as the observation point (r,z) in (16)–(19) or r in (21)–(24) is located outside the integration interval, every integral can be calculated by straightforward numerical integration. For so-called self-patch cases, where the observation point belongs to the integration interval, an integrand containing a singularity at the observation point has to be integrated. To this end, we determine the behavior of the integrand in the neighborhood of the observation point. Subtracting this behavior from the total integrand itself, we obtain a continuous function without any singularity which can easily be integrated numerically. The remaining term, i.e., the isolated singularity, can then be calculated analytically. As a matter of fact, the behavior of a function at a singularity can be found by developing the function as a Laurent series around the singularity. The self-patch problems of the coefficients in (15) are relatively easy since the singularity is of the first order. The problems related to the coefficients in (20), however, are much more complicated because of the higher order of the self-patch singularities that occur. For conciseness, no details will be given of these self-patch calculations.

The capacitance of the via is given by

$$C=-\frac{2\pi\epsilon d}{\ln\dfrac{r_1}{r_2}}-\sum_{n=1}^{P}4\pi\epsilon r_1 A_n\sinh\left(\alpha_n\frac{d}{2}\right)F_{1n}(r_1,r_1) + \sum_{i=0}^{N-1}2\pi\left(\frac{r_1}{N}\right)^2(2i+1)\frac{\tau_i}{V}+\sum_{j=0}^{M-1}4\pi r_1\frac{h}{M}\frac{\sigma_j}{V} \tag{25}$$

where

$$F_{1n}(v,w)=Y_1(\alpha_n v)J_0(\alpha_n w)-J_1(\alpha_n v)Y_0(\alpha_n w). \tag{26}$$

The first two terms are the contribution of the charges at the hole (region II); the last two terms are the contributions of the discretized surface charges above and under the ground plane (regions I and III).

VI. Numerical Results

We took $N=10$, $M=20$, and $L=2$ to 5, depending on the convergence. The thickness of the ground plane is $d=0.035$ mm and $\epsilon_r=4$. This will remain unchanged in all the examples presented in this section, except for the last example, where d will be varied. The computation time is about 3.5 min on a DEC-station 3100.

In Fig. 4, the capacitance of the via hole is shown as a function of its height, h, for a via radius $r_1=0.2$ mm and for several values of the radius r_2 of the ground plane opening. In order to display the numerical results in a clear way, we have divided the results over two figures. The capacitance increases sharply for $r_2\to r_1$, i.e., when the ground plane comes very close to the via.

Fig. 5 shows the equipotential lines for the case $h=0.4$ mm, $r_2=0.4$ mm, and $r_1=0.2$ mm. Only a quarter of the total cross section is shown.

The capacitance of the geometry shown in Fig. 1 is the sum of a contribution C_{II} in region II and contributions C_I and C_{III} in regions I and III. Owing to the symmetry of the problem, $C_I=C_{III}$. C_{II} is the capacitance generated by the finite thickness of the ground plane and is given by the first two terms of (25). C_I+C_{III} is given by the last two terms of (25). The ratio

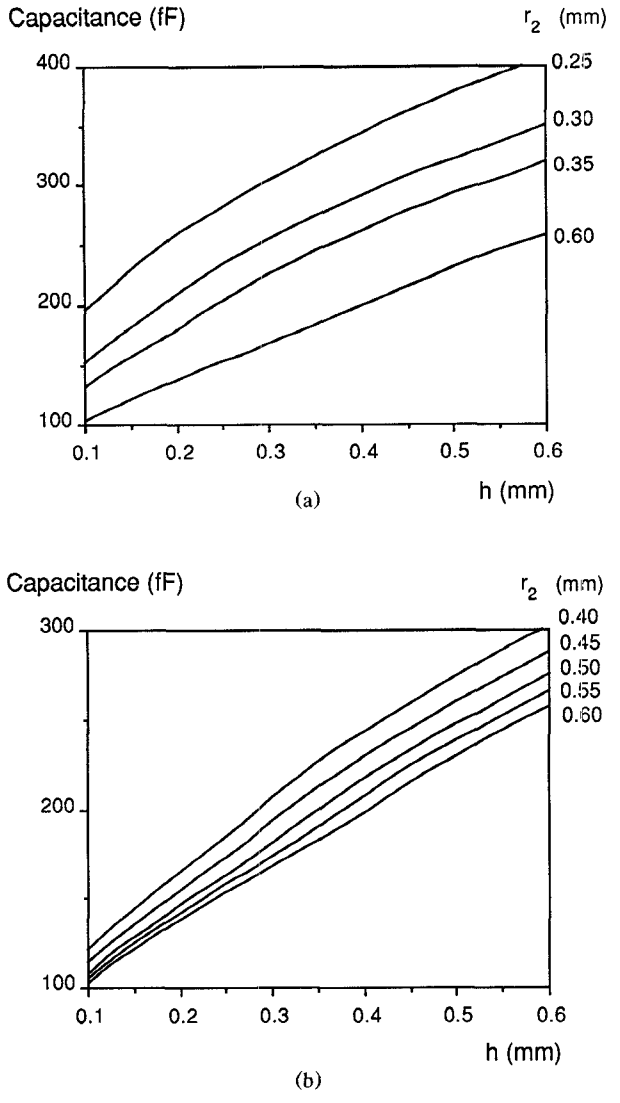

Fig. 4. Via hole capacitance as a function of its height and for different radii of the ground plane opening ($d = 35$ μm, $\epsilon_r = 4$, $r_1 = 200$ μm).

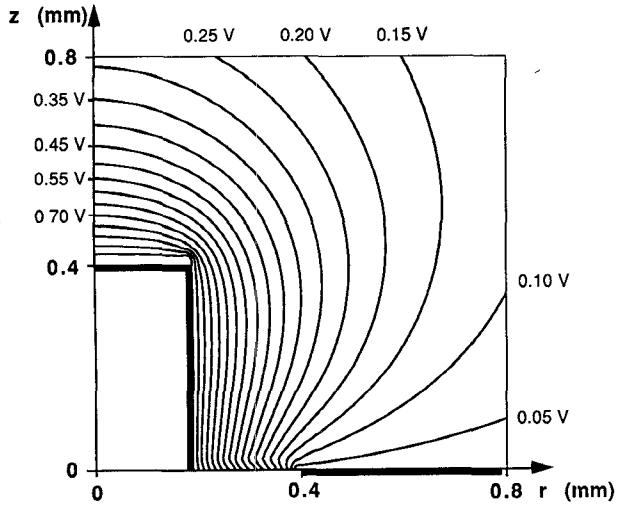

Fig. 5. Equipotential lines ($r_1 = 200$ μm, $r_2 = 400$ μm, $h = 400$ μm, $d = 35$ μm, $\epsilon_r = 4$).

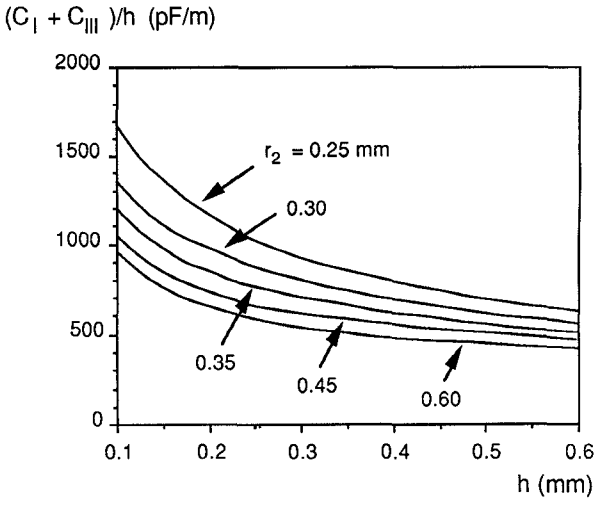

Fig. 6. Ratio of the part of the via hole capacitance outside the ground plane opening to its height as a function of the height ($d = 35$ μm, $\epsilon_r = 4$, $r_1 = 200$ μm).

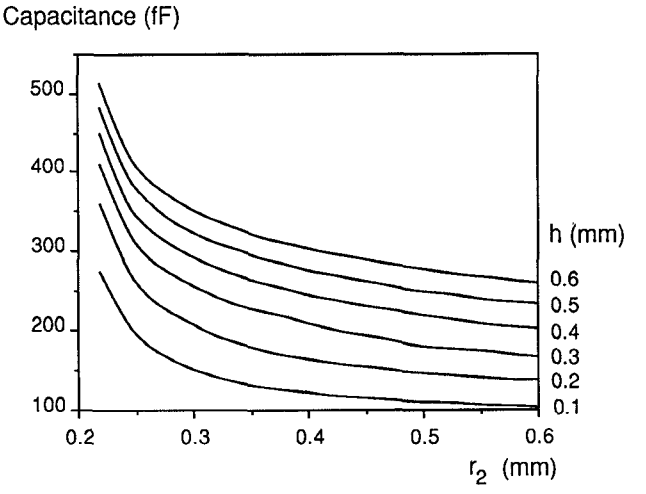

Fig. 7. Via hole capacitance as a function of the radius of its ground plane opening for different heights ($d = 35$ μm, $\epsilon_r = 4$, $r_1 = 200$ μm).

between $C_I + C_{III}$ and the height h gives an indication of the degree of linearity between the capacitance component above the ground plane and the height. In Fig. 6, this ratio is shown as a function of h for a via radius $r_1 = 0.2$ mm and for several values of r_2. From the data in Fig. 6, one can show that $C_I + C_{III}$ is approximately proportional to the square root of h.

In Fig. 7, the influence of the ground plane opening is displayed for a constant via radius $r_1 = 0.2$ mm and for several values of h. In Fig. 8 we have plotted the value of C_{II} for the example of Fig. 7 (solid line). For the given range of h values ($h = 0.1$ mm $\rightarrow h = 0.6$ mm) all curves coincide within the accuracy of the figure, showing that C_{II} is virtually independent of h. We examined the influence of changing the ground plane thickness d on this effect. Numerical results clearly indicate that our statement remains true if h is more than five times larger than d. The dotted curve shows the capacitance of the hole if it were a simple cylindrical capacitor with height d. As expected, the difference with C_{II} is not large. Fig. 9 shows the ratio between C_{II} and the total capacitance C, indicating the relative impor-

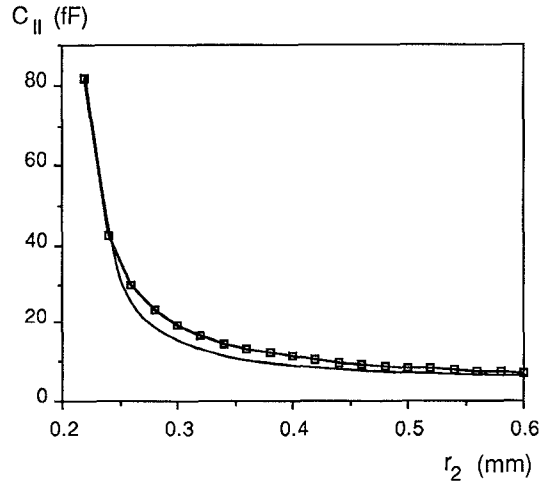

Fig. 8. Solid line: part of the via hole capacitance caused by the ground plane opening as a function of the radius of the ground plane opening ($d = 35$ μm, $\epsilon_r = 4$, $r_1 = 200$ μm). Dotted line: capacitance of a cylindrical capacitor with height d, inner radius $= r_1$, outer radius $= r_2$, and dielectric constant $= \epsilon_r$ as a function of r_2.

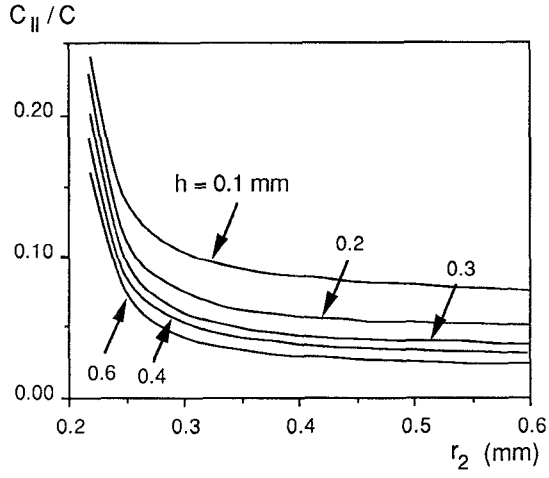

Fig. 9. Ratio of the ground plane opening capacitance to the total capacitance as a function of the radius of the ground plane opening ($d = 35$ μm, $\epsilon_r = 4$, $r_1 = 200$ μm).

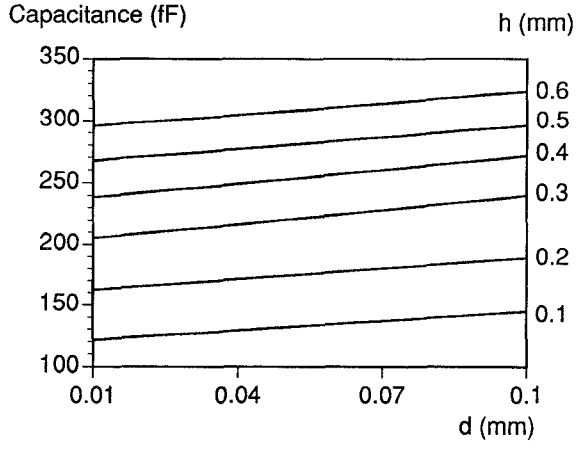

Fig. 10. Via hole capacitance as a function of the ground plane thickness for different heights ($\epsilon_r = 4$, $r_1 = 200$ μm, $r_2 = 400$ μm).

tance of the charge accumulation at the passage through the ground plane for the example of Fig. 7.

Finally, the influence of the ground plane thickness, d, is examined. In Fig. 10, the via capacitance is plotted as a function of d with $r_1 = 0.2$ mm and $r_2 = 0.4$ mm for several values of h.

The numerical results of our simplified approach have been compared with measurement data. For via holes in multiwire boards, we measure 0.1 to 1.5 pF per via hole for a board with four signal layers, four reference planes, and a thick metal core in the middle [11]. This confirms that our results lead to realistic values of the via capacitance.

VII. Conclusion

Combining an integral equation method with an analytical solution at the ground plane opening, we have calculated the capacitance of a simplified model of a via hole, taking into account the finite ground plane thickness. For realistic values of the geometrical parameters, it has been shown that the capacitance consists of two contributions. A first contribution comes from the part of the via hole above and below the ground plane. To a good accuracy this contribution is proportional to the square root of the height of the via. The second contribution comes from the finite thickness of the ground plane. For the considered range of geometrical values, its value is nearly independent of the height of the via. We have also compared this value with the one obtained by considering the hole in the ground plane an ideal cylindrical capacitor and found that the difference between the two values was rather small.

References

[1] T. Itoh, *Numerical Techniques for Microwave and Millimeter-Wave Passive Structures*. New York: Wiley, 1989.

[2] E. Sugita and O. Ibaragi, "Reliable multiwire circuits with small gauge wires," *IEEE Trans. Components, Hybrids, Manuf. Technol.*, vol. CHMT-2, pp. 532–536, Dec. 1979.

[3] G. Messner, "Cost–density analysis of interconnections," *IEEE Trans. Components, Hybrids, Manuf. Technol.*, vol. CHMT-10, pp. 143–151, June 1987.

[4] S. Papatheodorou, R. F. Harrington, and J. R. Mautz, "The equivalent circuit of a microstrip crossover in a dielectric substrate," *IEEE Trans. Microwave Theory Tech.*, vol. 38, pp. 135–140, Feb. 1990.

[5] W. Veit, H. Diestel, and R. Pregla, "Coupling of crossed planar multiconductor systems," *IEEE Trans. Microwave Theory Tech.*, vol. 38, pp. 265–269, Mar. 1990.

[6] T. Wang, R. F. Harrington, and J. R. Mautz, "The equivalent circuit of a via," *Trans. Soc. Comput. Simulation*, vol. 4, pp. 97–123, Apr. 1987.

[7] T. Wang, J. R. Mautz, and R. F. Harrington, "The excess capacitance of a microstrip via in a dielectric substrate," *IEEE Trans. Computer-Aided Design*, vol. 9, pp. 48–56, Jan. 1990.

[8] T. Wang, R. F. Harrington, and J. R. Mautz, "Quasi-static analysis of a microstrip via through a hole in a ground plane," *IEEE Trans. Microwave Theory Tech.*, vol. 36, pp. 1008–1013, June 1988.

[9] E. Durand, *Électrostatique*, vol. II: *Problèmes Généraux Conducteurs*. Paris: Masson, 1966, pp. 368–370.

[10] I. S. Gradshteyn and I. M. Ryzhik, *Table of Integrals, Series and Products*. New York: Academic Press, 1965, pp. 904–905.

[11] M. Botte, L. Van Hauwermeiren, D. De Zutter, and M. Herreman, "Differences between the multiwire and the multilayer technology for applications in high-frequency/high-speed systems," in *Proc. Fourth Conf. Electronic Packaging and Interconnections* (Milan), Oct. 1–2, 1990, p. 162.